Hindawi
Journal of Chemistry
Volume 2022, Article ID 3193689, 11 pages
https://doi.org/10.1155/2022/3193689

Research Article

Bioprospecting of an Endolichenic Fungus *Phanerochaete sordida* Isolated from Mangrove-Associated Lichen *Bactrospora myriadea*

Ramani H. Weerasinghe[1], **Chaitrali D. Shevkar**[2], **Kasun Maduranga**[1], **Komal H. Pandey**[2], **Renuka N. Attanayake**[3], **Abhijeet S. Kate**[2], **Gothamie Weerakoon**[4], **Santosh K. Behera**[2], **Kiran S. Kalia**[2], **and Priyani A. Paranagama**[1]

[1]*Department of Chemistry, University of Kelaniya, Kelaniya 11600, Sri Lanka*
[2]*National Institute of Pharmaceutical Education and Research, Ahmedabad 382355, India*
[3]*Department of Plant and Molecular Biology, University of Kelaniya, Kelaniya 11600, Sri Lanka*
[4]*Algae, Fungi and Plants Division, Department of Life Sciences, The Natural History Museum, Cromwell Road, London SW7 5BD, UK*

Correspondence should be addressed to Priyani A. Paranagama; priyani@kln.ac.lk

Received 21 December 2021; Revised 14 March 2022; Accepted 15 March 2022; Published 16 April 2022

Academic Editor: Josefina Pons

Bioassay-guided fractionation of the ethyl acetate extract of *Phanerochaete sordida*, an endolichenic fungus (ELF) isolated from the host lichen *Bactrospora myriadea*, collected from Negombo lagoon, Sri Lanka, led to the isolation of a bioactive compound. Following the identification of the fungus using morphological and DNA barcoding techniques, the pure compound was isolated using column chromatography, preparative TLC, and semipreparative HPLC. The structure elucidation was carried out using IR, HR-ESI-MS and ^{1}H, ^{13}C & 2D NMR spectroscopic methods. The *in vitro* bioassays conducted revealed that compound 1 has a high antioxidant activity with $ABTS^{\bullet+}$ (IC_{50}58.91 ± 1.35 μM), moderate anti-inflammatory activity (IC_{50}254.79 ± 1.41 μM), comparable antibacterial activity against the oral-bacterial strain *Streptococcus mutans* (MIC 898.79 μM and MLC 1797.58 μM), moderate tyrosinase inhibition (IC_{50}1713.69 ± 8.65 μM), and moderate cytotoxicity against oral cancer (IC_{50}13.65 ± 0.02 μM), in comparison with respective positive controls. The *in silico* experiments conducted for tyrosinase inhibition and cytotoxicity using Schrödinger revealed results in line with the *in vitro* results, thus confirming the bioactivities. The molecule also satisfies the key features of drug likeliness according to pharmacokinetic studies.

1. Introduction

Endolichenic fungi (ELF), asymptomatic fungal associates which live in the interior of a lichen thallus, serve as an incredible source of novel bioactive compounds. While adding evidence in proving lichens to be "cradles of fungal diversification" [1], this distinct group of fungi has been found to produce compounds with antioxidant, antibacterial, anti-inflammatory, antifungal, anticancer, and numerous other potentials [2]. Subsequent to the first report of such isolated compounds in 2007 [3], more than 172 compounds have been isolated and explored from ELF while more than 99 of them had been novel molecules [4]. Experiments conducted in Sri Lanka revealed numerous such potent compounds, which include polyketides from ELF *Penicillium citrinum* [5] and *Curvularia trifolli* [6] along with more metabolites from *Daldinia eschscholtzii* [7] *Xylaria psidii* [8], and *Neurospora ugadawe* [9].

The ELF used in the present study, *Phanerochaete sordida*, was isolated from the host lichen *Bactrospora*

myriadea, collected from the mangrove ecosystem of Negombo lagoon, Sri Lanka, in early March, 2018. This particular strain is known to degrade the lignin, cellulose, and hemicellulose [10]. *Phanerochaete sordida* is a member of the division basidiomycete and subjected for further studies since not many ELF from this division are reported. It was hypothesized that if a basidiomycete survives as an ELF, it should be metabolically unique. A thorough literature survey revealed that this is the first report of isolation of a bioactive compound from *P. sordida*.

The aim of the present study was to bioprospect and conduct compound isolation on the ethyl acetate extract of the ELF *P. sordida* using bioassay-guided fractionation and investigate their bioactive potentials using *in vitro* and *in silico* techniques. The compound was identified using spectroscopic data. The *in vitro* assays were conducted to evaluate the antioxidant, anti-inflammatory, tyrosinase inhibitory, antibacterial, and cytotoxic potentials of the compound. *In silico* approach was used in tyrosinase inhibitory and cytotoxic screenings, to establish the validity of the obtained *in vitro* results. Following the widely used trend of molecular docking, interactions of the compound with selected receptors in cancer cells and tyrosinase enzyme were assessed using Schrödinger (2021-1) software. Molecular docking has improved the drug discovery process by providing estimations of a compound's affinity to receptors and thereby expediting the lead optimization processes [11]. Furthermore, pharmacokinetic studies were carried out to assess the perfect balance between high biological activity and low toxicity. The ADMET (Absorption, Distribution, Metabolism, Excretion and Toxicity) parameters which comprehensively address the chemical drug-likeness of the compound were assessed using the freely accessible SwissADME web tool [12]. This comprehensive report contains the details of preliminary identification and screening for biological activities of the fungus combined with the isolation, identification, bioactivity screening, and computational studies of the isolated compound.

2. Materials and Methods

2.1. Ethical Statement. Permit to collect lichen samples from the mangrove forest in Negombo lagoon was obtained by the Forest Department of Sri Lanka. The samples were collected from mangrove and mangrove-associated plants in the area of "Kadolkele" under the observation of a representative of the department, without causing any disturbance to the surroundings.

2.2. Collection of Lichen Sample. Lichen host was collected on the 31st of March, 2018, at the mangrove forest of Negombo lagoon, Sri Lanka. The study site was "Kadolkele" area situated at 7.195528 N 79.84389 E GPS coordinates belonging to the Negombo lagoon area in Sri Lanka. Sample was immediately placed in an acid free paper bag, labeled appropriately, and transported to the Department of Chemistry, University of Kelaniya, and stored in 4°C to be processed for the isolation of ELF within two weeks of sampling.

2.3. Lichen Identification. A portion of lichen of the particle (2×2 cm) was air-dried for two weeks and refrigerated. The identification of this lichen was carried out using morphological and molecular techniques at Natural History Museum, London, and photographs were taken using Olympus stereomicroscopes and Olympus compound microscopes with interference contrast, connected to a Nikon Coolpix digital camera. Tap water was utilized for section mounting for all measurements [9]. Duplicate of the specimen was deposited in the Department of Chemistry, University of Kelaniya.

2.4. Isolation of Endolichenic Fungi. Lichen thallus was washed in running tap water to remove unwanted particles and then surface sterilized using consecutive immersion in 96% ethanol for 10 s, 0.5% sodium hypochlorite for 2 min, and 70% ethanol for 2 min and dried using sterile filter paper. Small segments of the lichen thallus (approximately 3 $\times$ 3 mm) was then cut and placed on 2% malt extract agar (MEA) supplemented with 0.01% streptomycin (Sigma-Aldrich). Sealed plates were then incubated under ambient conditions (room temperature 30°C) for 14 days and observed regularly. Hyphal tips from each morphologically distinct colony was placed in new PDA plates and subjected to several subculturing to obtain a pure culture [3]. Among various fungal isolates, a sterile and fast-growing basidiomycete isolate was selected for further studies since isolation of basidiomycetes as ELF is as not as frequent as ascomycetes.

2.5. Extraction of Genomic DNA and Polymerase Chain Reaction (PCR). The isolate was inoculated in Potato Dextrose Broth (PDB) and incubated at room temperature (30 ± 32°C) for one week. Mycelia were separated from the broth, washed with sterilized water, and remove excess water, and DNA was extracted using a slightly modified method of CTAB DNA extraction protocol [13]. Quality of extracted DNA sample was tested using 1% agarose gel electrophoresis, and sample was stored at -20°C for further utilization. The nuclear ribosomal internal transcribed spacer region (rDNA-ITS) was amplified using polymerase chain reaction (PCR); using the fungal-specific ITS5 forward and ITS4 reverse universal primers [14]. The PCR reaction procedure was conducted as described in Maduranga et al. (2018)[15] Clean PCR products were subjected to bidirectional Sanger dideoxy sequencing at Genetech Institute, Colombo, Sri Lanka. DNA sequences were manually edited using BioEdit sequence alignment editor (Version 7.2.5) and compared with the sequences available in the GenBank using Basic Local Alignment Search Tool (BLAST) to assess homology. The isolated fungus was identified comparing sequence of ITS-rDNA region with the established (voucher specimens or published) records with the highest percent similarity of the GenBank accessions. DNA sequence of the identified ELF species was deposited at the NCBI database, and an accession number was obtained [9].

2.6. Extraction and Isolation of Secondary Metabolites from the Endolichenic Fungus. The ELF was cultured on PDA plates of 150 mm diameter (100 plates) and incubated at room temperature for 2 weeks. The mycelium with the

medium were cut into small pieces, extracted to ethyl acetate (6 × 500 mL), and the solvent was evaporated under reduced pressure using the Rotary Evaporator (IKA RV 10B S96, Germany). The evaporated ethyl acetate extract was then transferred to a glass vial separately, and N_2 gas was passed through the sample to remove any remaining solvent. The resulting semisolid extract was stored at 0°C for further analysis [5].

2.7. Bioassay-Guided Isolation of the Compound. Since the ethyl acetate extract showed significant antioxidant, antibacterial, and anti-inflammatory activity, 5.84 g of the crude extract was partitioned with hexane, chloroform, and methanol, in order to separate nonpolar, moderately polar, and polar compounds, respectively. The chloroform fraction (4.2 g) was found to possess the highest activity in antioxidant, antibacterial, and anti-inflammatory assays. Hence, it was subjected to column chromatography using normal phase silica gel. The column (70-230 mesh, 19.0 g, 2 cm × 50 cm) was eluted with 100% chloroform containing increasing amounts of methanol and finally methanol. The collected fractions were combined according to thin layer chromatography (TLC) profiles to yield 7 major fractions (F1–F7). Of the seven fractions, F1 (38.7 mg) and F2 (314.5 mg) contained the same major compound and were subjected to column chromatography with the same polarity gradient. Column fractions obtained from F1 and F2 were combined after running the TLC and purified using preparative TLC (PTLC) to afford two fractions of the same pure compound, compound 1 (weights: 7.0 and 11.7 mg). After utilizing a portion to perform bioassays (please note that cytotoxicity assay was conducted after the final purification), the remaining of the fractions were sent to obtain spectral data. The combined fractions were further purified using preparative HPLC with a semipreparative column (Waters, Xterra Prep RP C_{18} column, 5 μm, 19 × 150 mm) applying the following method: (A) 1% formic acid in deionized water and (B) methanol, gradient; 95% A/5% B (0 min), 95% A/5% B (5 min), 5% A/95% B (15 min), 5% A/95% B (25 min), 95% A/5% B (28 min), and 95% A/5% B (30 min); flow rate 5 mL/min. One pure compound (compound 1, weight: 4 mg) was isolated, and the structure of the compound was determined by ^{1}H-NMR and ^{13}C-NMR spectroscopy (Bruker, 500 MHz in $CDCl_3$) in combination with DQF-COSY, DEPT, HMBC, HSQC, and NOESY correlations. Molecular mass of the compound 1 was obtained using HR-ESI-MS.

2.8. Radical Scavenging Ability by (2,2′-Azino-Bis(3-Ethylbenzothiazoline-6-Sulfonic Acid)) ($ABTS^{\cdot+}$) Method. The radical scavenging ability assay was carried out in a flat bottom 96-well microtiter plate, according to the method described by [16] with slight modifications. Different doses of the test sample and standard antioxidant, butylated hydroxy-toluene (BHT) (0.0, 15.62, 31.25, 62.5, 125.0, 250.0, 500.0, and 1000.0 μg/mL) was added (10 μL) to 190 μL of freshly prepared ABTS solution in the 96 well plate. All reagents were mixed and incubated for 7 min at room temperature under dark conditions. The absorbance of each well was measured at 714 nm with a Microplate Reader (Biotek, USA). The percentage inhibition was calculated using the Equation (1), where control is the absorbance of the control sample and the sample is the absorbance of the treatment. The IC_{50} values were calculated using GraphPad Prism 7.04. The experiment was carried out in triplicates.

$$\%\text{Activity} = \frac{A_{\text{control}} - A_{\text{sample}}}{A_{\text{control}}} \times 100\%. \quad (1)$$

2.9. Anti-Inflammatory Assay (HRBC Stabilization Method). The anti-inflammatory assay was conducted using human red blood cell stabilization method which uses the heat induced hemolysis principle [17]. Test sample and the positive control aspirin (1 mg of each) were dissolved in 0.5 mL of DMSO (dimethyl sulfoxide) and diluted up to 5 mL by addition of normal saline. A half dilution series was prepared with a control, and the reaction mixture was prepared with 2.5 mL of the solution and 0.25 mL of 10% *v*/*v* RBC suspension. All the centrifuge tubes containing reaction mixtures were incubated in a water bath at 56°C for 30 min after which the tubes were cooled under running tap water. The reaction mixture was centrifuged at 3000 rpm for 10 min to obtain a clear liquid phase, and the absorbance of the supernatants was measured at 560 nm using Microplate Reader (Biotek, USA) by using aliquots of 200 μL for each well in a 96 well-plate from each mixture. The test was performed in triplicates, and the percentage stability was calculated using Equation (1). IC_{50} values were calculated using the statistical software GraphPad Prism 7.04.

2.10. Tyrosinase Inhibitory Assay. Tyrosinase inhibitory assay was carried out in a flat bottom 96-well microtiter plate according to a modified version of [18]. Test sample and positive control Kojic acid were dissolved in 10% DMSO in phosphate buffer (pH 6.5), and a half dilution series of doses was prepared for each (0.0, 10.41, 20.83, 41.66, 83.33, 166.60, and 333.30 μg/mL). An aliquot of 70 μL of each dilution was combined with 30 μl of tyrosinase (333 U/mL). Followed by an incubation at room temperature for 5 min, 110 μL of substrate (2 mM L-DOPA) was added to each well, incubation was continued for 30 min at room temperature under dark conditions, and absorbance was measured at 490 nm with a Microplate Reader (Biotek, USA). The percentage inhibition was calculated using Equation (2)

$$\%\text{Inhibition} = \frac{\left(A_{\text{control}} - A_{\text{blank}}\right) - \left(A_{\text{sample}} - A_{\text{blank}}\right)}{\left(A_{\text{control}} - A_{\text{blank}}\right)} \times 100\%. \quad (2)$$

2.11. Antibacterial Assay (Agar Well Diffusion Method). Antibacterial assay against the anaerobic bacterial strain *Streptococcus mutans* (ATCC 700610) was conducted using agar well diffusion method [19]. An aliquot of overnight cultures in Trypticase soy broth (supplemented with blood with lysed RBC and grown under anaerobic conditions in a jar containing anaerobic sachets at 37°C) was diluted hundred times, and a quantity of 100 μL was spread evenly on the

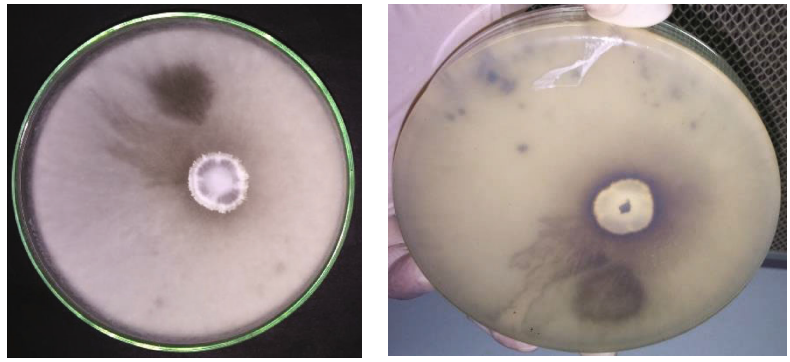

(a) (b)

Figure 1: Culture of *P. sordida* on PDA after 7 days of inoculation: (a) front side; (b) rear side.

surface of the Trypticase soy agar (supplemented with lysed RBC) plates prepared. Wells with a diameter of 0.5 cm were made on the plates using a cork borer. Sample and chlorhexidine (0.2%) (positive control) were dissolved in DMSO to meet 5 mg/mL concentration for initial screening. In order to determine minimum inhibitory concentration (MIC) and minimum lethal concentration (MLC) of the compound 1, a concentration series of 1000, 750, 500, 250, 100, 50, and 10 μg/mL was utilized. The wells were filled with 100 μL of the test solutions while keeping a negative control of DMSO. After an incubation of 24 hours at room temperature under anerobic conditions, the diameters of observable inhibition zones were measured in mm [20].

2.12. Cytotoxicity Assay (Alamar Blue Method). Cytotoxicity was determined using the Alamar Blue assay with slight modifications [21] against the cell lines of CAL-27 (Oral cancer). Cell seeding was done using a concentration of 5000 adherent cells per well in a 96 well plate. After a 24 hr incubation period, the wells were treated with 100 μL of compound (a concentration series of 1, 5, 10, and 20 μM in triplicates). Followed by another 24 hr incubation period, 100 μL of Alamar Blue solution in 1X PBS (phosphate-buffered saline) was added to each well. After a period of 4 hr, the fluorescence was measured using Varioscan Go instrument with ScanIt software at 510 nm (excitation) and 519 nm (emission). Doxorubicin was used as the positive control to compare the results. The results were calculated using Equations (3) and (4) analyzed using statistical software GraphPad Prism 7.04.

$$\%\text{Proliferation} = \frac{\left(A_{\text{sample}} - A_{\text{blank}}\right)}{\left(A_{\text{control}} - A_{\text{blank}}\right)} \times 100\%, \quad (3)$$

$$\%\text{Inhibition} = 100 - \%\text{Proliferation}. \quad (4)$$

2.13. In Silico Studies. Protein sequences were retrieved from Universal Protein Resource (UniProtKB) database, and homology modelling was used accordingly to select and retrieve protein structures representing CAL-27 (oral cancer) cell lines and tyrosinase enzyme. Rho-associated protein kinase (ROCK 1), programmed cell death 6-interacting protein (ALIX) [22], and tumor susceptibility gene 101 protein (TSG101) [23] were selected as receptors for CAL-27 cell. Molecular details were obtained from UniProtKB database with UniProt ID Q13464, Q8WUM4, and Q99816, respectively. The protein structures were obtained from RCSB (Research Collaboratory for Structural Bioinformatics), PDB (Protein Data Bank) with ID 2ETR, 3C3R, and 3OBQ having 2.60 Å, 2.02 Å, and 1.40 Å resolutions, respectively. For tyrosinase enzyme, the enzyme itself was selected as the suitable receptor in line with UniProt ID P1469, and structure was obtained from ModBase. Please note that the structures retrieved for cell lines and tyrosinase enzyme were from human sources.

Binding pocket prediction was conducted utilizing CASTp and Ghecom for 2ETR, 3C3R, 3OBQ, and tyrosinase. The compound was docked against all selected proteins using the docking software Schrödinger (2021-1). Grids were generated for each of the protein with following amino acids: (a) 2ETR: Met 156, Ile 82, Phe 368, Leu 205, Val 90, Asp 202, Tyr 155, Met 153, Glu 154, Ala 103, Ala 205, Asp 216, and Asn 203; (b) 3C3R: Glu 137, Asp141, Ala 151, Tyr 153, Leu 201, Thr 204, Asp 206, Pro 238, Ile 251, Asn 255, Val 297, Phe 300, and Lys 303; (c) 3OBQ: Thr 58, Arg64, Asn 66, Tyr 68, Asn 69, Lys 98, Thr 92, Met 95, Phe 142, and Ser143; (d) tyrosinase: His 19, Gln 68, Val 74, Asp 76, Phe 84, Gly 154, Met 159, Tyr 181, Leu 188, Arg 196, His 202, Leu 288, Thr 309, Ala 357, His 363, Ile 396, Pro417, and His 420. Resultant docking complex was evaluated for ligand efficiency, binding energy scores, and intermolecular H-bonds.

The drug likeliness and pharmacokinetic profile of the compound were studied using SwissADME tool.

3. Results and Discussion

3.1. Identification and Isolation of Endolichenic Fungus. The lichen was collected from the mangrove plant *Rhizophora mucronata*, a true mangrove species among one of the frequently found plant species in the mangrove ecosystem of Negombo lagoon, Sri Lanka [24]. The lichen host of the ELF isolate was identified using morphological and molecular techniques as *Bactrospora myriadea*. The obtained ITS sequence of the ELF sample showed 98.5% sequence homology to *Phanerochaete sordida* sequence submitted by Kamei

Table 1: Summary of bioactivities of crude extracts and partitions of *Phanerochaete sordida*.

	ABTS assay Activity at highest concentration of 50 μg/mL (%)	HRBC stabilization assay IC_{50} value (μg/mL)	Tyrosinase inhibitory assay Activity at highest concentration of 666.67 μg/mL (%)	Antibacterial assay against *S. mutans* Inhibition zone diameter (mm)
Crude extract	34.13 ± 0.62	124.00 ± 0.45	12.58 ± 0.37	16 ± 0.15
Hexane partition	24.57 ± 0.22	170.27 ± 3.02	22.54 ± 0.97	—
Chloroform partition	43.17 ± 0.55	88.62 ± 0.76	42.42 ± 0.50	11 ± 0.04
Methanol partition	13.95 ± 3.76	Max < 50%	9.91 ± 1.28	—

Three replicates were used in each assay, and the values are given with ±standard error. Max < 50% indicates that activity showed by the maximum dosage did not surpass 50%.

Table 2: ^{13}C and ^{1}H NMR data for the compound 1 in $CDCl_3$.

Position	δ 13C	δ 1H (multiplicity, nH, J/Hz)	DEPT
1	20.11	1.36 (d, 3H, 5)	CH_3
2	21.16	1.48 (m, 2H)	CH_2
3	24.12	1.48 (m, 2H)	CH_2
4	24.68	1.61 (m, 2H)	CH_2
5	27.24	1.55 (m, 2H)	CH_2
6	30.78	1.61 (m, 2H)	CH_2
7	31.08	1.79 (m, H) 1.92 (m, H)	CH_2
8	33.54	2.50 (m, H) 3.28 (m, H)	CH_2
9	75.17	5.17 (m, H)	CH
10	101.37	6.28 (d, H, 2)	CH
11	105.56 (quaternary)		
12	110.80	6.23 (d, H, 2)	CH
13	149.48 (quaternary)		
14	160.08 (quaternary)		
15	165.34 (quaternary)		
16	171.90 (quaternary)	12.00 (OH)	

et al. [25] (accession number AB210078.1) in GenBank. The obtained sequence was deposited under the accession number MT507808 in the GenBank. The isolate showed rapid growth on PDA, covering a 150 mm diameter petri-dish within two weeks. The colony colour was white to grey by the second week after incubation at the room temperature (Figure 1).

3.2. In Vitro Assays. As per bioassay-guided fractionation, the *in vitro* assays were first conducted (except anticancer assay) to the ethyl acetate crude extract followed by hexane, chloroform, and methanol partitions. According to the results, the chloroform partition was subjected to further isolation owing to its highest activity compared to the others. The comparison of results is presented in Table 1.

Bioassay-guided fractionation of the chloroform fraction using column chromatography, PTLC, and preparative HPLC yielded pure compound 1, and the bioactivity of the compound 1 was evaluated using the *in vitro* bioassays.

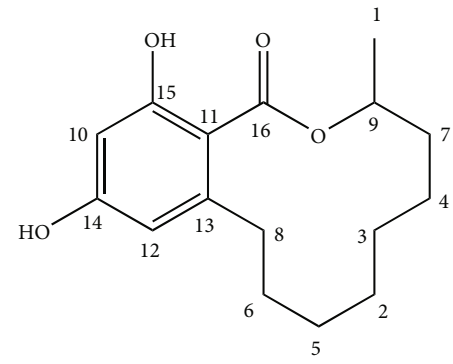

Figure 2: The structure of the compound 1.

3.3. Structure Elucidation. Bioassay-guided fractionation of the ethyl acetate extract of *P. sordida* yielded the compound as a white-coloured solid. The compound gave $[M+H]^+$ ion in the high-resolution electrospray ionization mass spectrometry

Table 3: *In vitro* assay activity comparison of the compound 1 with respective positive controls.

In vitro assay	Activity of the compound 1	Activity of the positive control
ABTS assay	IC_{50}58.91 ± 1.35 μM	IC_{50}55.20 ± 4.04 μM
HRBC stabilization assay	IC_{50}254.79 ± 1.41 μM	IC_{50}134.16 ± 1.33 μM
Tyrosinase inhibitory assay	IC_{50}1713.69 ± 8.65 μM	IC_{50}148.43 ± 13.04 μM
Antibacterial assay	MIC 898.79 μM, MLC 1797.58 μM	MIC 98.92 μM, MLC 197.85 μM
Anticancer assay against oral cancer	IC_{50}13.65 ± 0.02 μM	IC_{50}01.20 ± 0.03 μM

Three replicates were used in each assay and the values are given with ±standard error.

Table 4: Molecular docking scores of compound 1 against selected proteins.

Sr. no	Protein	PDB ID	Binding energy (kcal/Mol)
1	Rho-associated protein kinase 1	2ETR	-5.642
2	ALIX	3C3R	-4.878
3	TSG101	3OBQ	-4.641
4	Tyrosinase	Structure obtained from ModBase	-5.234

(HR-ESI-MS) at *m*/*z* 279.1603, which was consistent with a molecular formula of $C_{16}H_{22}O_4$ (calcd.278.15186), requiring 6 sites of unsaturation. The absorption peaks appearing in the IR spectrum occurring at 3343 cm^{-1} (broad peak) and 1620 cm^{-1} (towards the lower end of carbonyl stretch due to the attached aromatic group) suggested the presence of hydroxyl and carbonyl groups, respectively. UV spectrum showed maximum absorption bands at 220 and 260 nm confirming the presence of a carbonyl group. With the attained information, a thorough search was done using SciFinder and Dictionary of Natural Products (DNP) using species and genus specific filters. Since no matches were found, structure elucidation was conducted using NMR data.

The aromatic region of the ^{1}H NMR spectrum exhibited two signals at δ_H 6.23(d, 2 Hz) and δ_H 6.28 (d, 2 Hz), and this spin system consisting of two 1H doublets was shown to be due to metacoupled protons with 2.2 Hz. The ^{13}C NMR signals at δ_C 101.37, 105.56, 110.80, 149.48, 160.08, and 165.34 completed the carbon skeleton of the aromatic ring. The carbon signal at δ_C 75.17 was indicative of a carbon connected to an oxygen with a single bond. The D_2O experiment carried out revealed significant lowering of intensity of the ^{1}H peaks at δ_H 5.53 and 12.00, affirming the protons as of hydroxyl groups. An analysis of the spectra ^{13}C NMR, DEPT, and HSQC revealed one methyl carbon (δ_C 20.11), seven methylene carbons (δ_C 21.16, 24.12, 24.68, 27.24, 30.78, 31.08, and 33.54), and one sp^3 methine carbon (δ_C 75.17) with the olefinic carbons in the aromatic ring mentioned above (δ_C 101.37 and 110.80). Four out of the five quaternary carbons were embedded in the aromatic ring at δ_C 105.56, 149.48, 160.08, and 165.34 with latter two being more deshielded due to each being bonded to an oxygen atom. An analysis of ^{1}H-^{1}H correlations observed in the DQF-COSY spectrum revealed the presence of CH_3 CH CH_2 and CH_2 CH_2 CH_2 isolated spin systems. The ^{1}H-^{1}H correlations observed in the DQF-COSY and HSQC further indicated that two Hs of carbons at δ_C 33.54 (δ_H 2.50 and 3.28) and δ_C 31.08 (δ_H 1.79 and 1.92) were nonequivalent methylene protons. In HMBC spectrum, the aromatic proton at δ_H 6.28 showed correlations with δ_C 105.56, 110.80, 160.08, and 165.34 while the proton at δ_H 6.23 showed correlations to the aromatic carbons at δ_C 101.37 and 105.56 as well as to the benzylic carbon at δ_C 33.54. The ^{13}C NMR spectrum of compound **1** when analyzed with the help of the HMBC and DEPT spectra showed the presence of a caboxylic carbonyl (δ 171.9), and it further indicates the correlation of the proton in carboxyl group at δ_H 12.00 with δ_C 101.37, 105.56, and 165.34. The HMBC correlations were observed from δ_H 1.36 to δ_C 75.17; δ_H 1.79 to δ_C 20.11; δ_H 1.92 to δ_C 24.12, and 75.17 with δ_H 1.48 long range coupling to δ_C 20.11. The NOESY correlations depict that the protons at δ_H 1.79, 5.53, and 12.00 are in close proximity to each other in spacial arrangement of the molecule. The structure of the compound 1 was thus elucidated as 12,14-dihydroxy-3-methyl-3,4,5,6,7,8,9,10-octahydro-1H-benzo[-c][1]oxacyclododecin-1-one.

The ^{1}H and ^{13}C NMR data pertaining to the structure elucidation is presented in Table 2, and the structure is shown in Figure 2.

Subsequent search in SciFinder of the elucidated structure revealed that this compound has previously been isolated firstly from the fungus *Lasiodiploidia theobromae* [26]. It is a member of the large group of resorcinylic acid lactones and is known as (R)-de-O-methyllasiodiplodin. This is the first time the compound has been isolated from the genus *Phanerochaete* until date.

This macrolide is previously known to be a nonsteroidal mineralocorticoid receptor antagonist and to possess a variety of bioactivities [27].

Here, we are presenting and discussing activities which have not been reported before for this compound. Activity comparison of the compound 1 with relevant positive controls for all the *in vitro* assays is presented in Table 3.

According to literature, the compound is known to reduce DPPH radical [28]. In this study, radical scavenging activity was assessed using the *in vitro* assay stated under

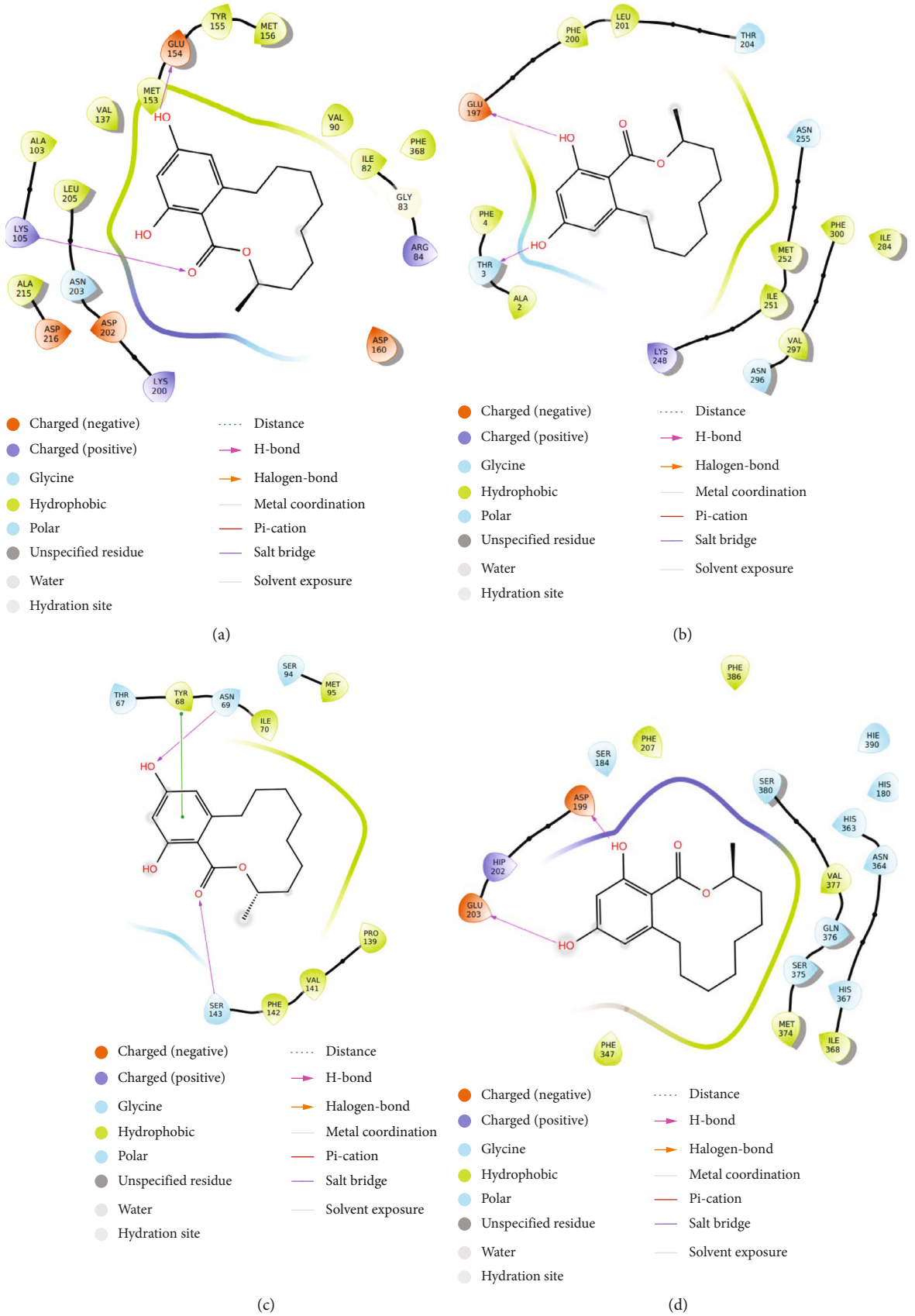

Figure 3: The 2D interactions of compound 1 with (a) 2ETR (b) 3C3R (c) 3OBQ, and (d) tyrosinase enzyme.

Table 5: Drug likeliness, physicochemical, and pharmacokinetic properties of compound 1.

Physicochemical properties	Pharmacokinetic properties	Drug likeliness
Molecular weight g/Mol 278.34	Gastro-intestinal (GI) absorption High	Lipinski—yes (0 violations)
Heavy atoms 20	Blood brain barrier (BBB) permeant Yes	Ghose—yes
Aromatic heavy atoms 6	P-gp substrate No	Veber—yes
H bond donar 2	CYP1A2 inhibitor No	Egan—yes
H bond acceptors 4	CYP2C19 inhibitor No	Muegge—yes
Fraction Csp3 0.56	CYP2C9 inhibitor Yes	Bioavailability score—0.55
Number of rotatable bonds 0	CYP2D6 inhibitor No	
Molar refractivity 78.27	CYP3A4 inhibitor No	
TPSA (topological polar surface area) 66.76 Å	Log K_p (skin permeation) -4.48 cm/s	
Consensus log $P_{o/w}$ 3.35		

methods against the radical monocation $ABTS^{\bullet+}$. As shown in Table 3, the close IC_{50} value shown by the compound 1 (IC_{50}58.91 ± 1.35 μM) to that of the positive control BHT (IC_{50}55.20 ± 4.04 μM) against $ABTS^{\bullet+}$ radical monocation displays promising antioxidant potential of the compound 1.

Compound 1 has been reported to inhibit the production of nitric oxide [29] and prostaglandin [30] which act as inflammatory mediators. Supportingly, in this study, the anti-inflammatory activity is assessed by the ability to stabilize the lysosomal membrane through HRBC stabilization assay. The activity shown by the compound 1 (IC_{50}254.79 ± 1.41 μM) is slightly comparable to the positive control aspirin (IC_{50}134.16 ± 1.33 μM). It could be assumed that binding mechanism of the compound 1 is not similar to that of aspirin (acetylsalicylic acid) though further studies are required to confirm its validity.

Inhibition of tyrosinase enzyme is the most convenient way of controlling melanogenesis, since it catalyzes the first and only rate-limiting step in the process. Hence, the demand for tyrosinase inhibitors has increased to solve the issue of hyperpigmentation [31]. This compound showed moderate activity compared to the commercially available inhibitor kojic acid. Further, *in silico* analysis was conducted to assess the binding of the compound to the enzyme, which will be discussed later in the manuscript.

The oral-bacterial strain *Streptococcus mutans*, known for its pathogenicity of dental caries, is now even proved to be a potential risk factor in causing systemic diseases such as ulcerative colitis [32]. In an era where the antibiotic resistance has become a major issue, even in oral health, emergence of compounds with promising antibacterial activity is vital [33]. The agar well diffusion method carried out to assess the antibacterial activity of the compound 1 with a series of concentrations as stated under methods section revealed that the minimum inhibitory concentration (MIC) and minimum lethal concentration (MLC) values of the compound 1 were 898.79 μM and 1797.58 μM, respectively. These MIC and MLC values were higher than that of the commercially available antibiotic chlorohexidine (MIC 98.92 μM, MLC 197.85 μM).

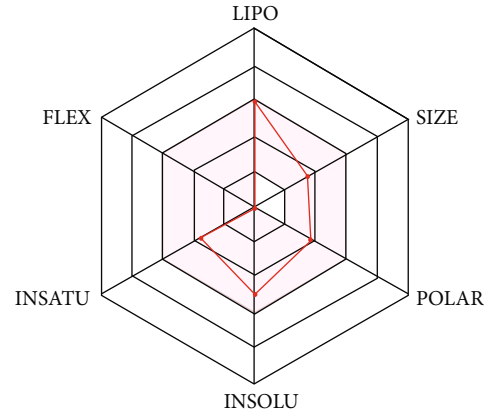

Figure 4: Bioavailability radar by SwissADME tool (Pink area in the figure represents optimal range of particular property) for compound 1. (LIPO: lipophilicity; SIZE: size as molecular weight; POLAR: polarity asTPSA; INSOLU: insolubility in water; INSATU: insaturation as per fraction of carbons in the sp3 hybridization; FLEX: flexibility as per rotatable bonds).

The burden of cancer and mortality is increasing at an alarming rate as per the global cancer statistics. Only in 2020, 19.3 million new cancer cases and almost 10.0 million cancer deaths have been reported worldwide. Among many

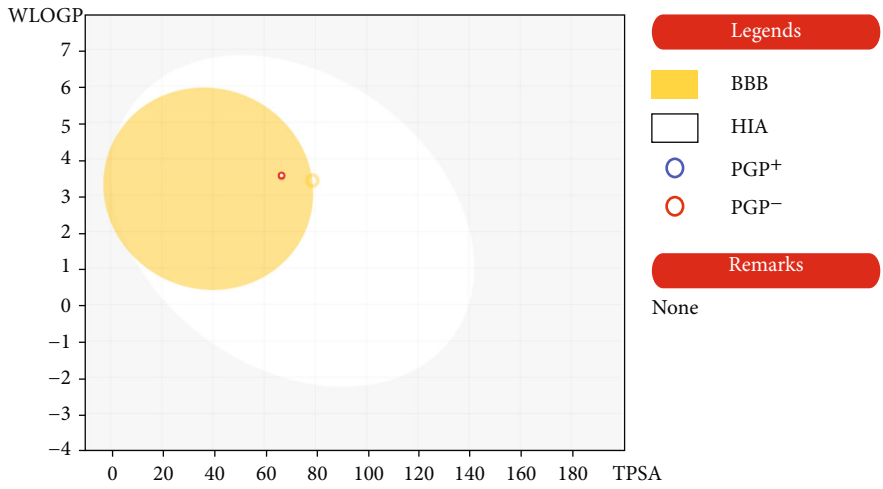

Figure 5: Predicted human intestinal absorption and blood brain permeability as per BOILED EGG diagram of compound 1.

others, tongue squamous cell carcinoma (tongue cancer) has been found to be one of the most common malignancies seen in the oral maxillofacial region [34]. In order to determine the anticancer potency of the compound 1 against oral cancer, the cell line CAL-27 (oral cancer) was used in Alamar Blue cell-culture assay. It seems to possess comparable activity against CAL-27 (IC_{50}13.65 ± 0.02 μM) cancerous cell line. The cytotoxicity on normal cells was assessed by using the normal breast cell line Mcf10a, and it was found to be nontoxic up to a concentration of 100 μM (Please note that maximum percentage of methanol used was 0.2 percent, which did not show any toxicity as per the vehicle control fluorescence observed.). Moreover, *in silico* studies were conducted to determine interactions of the compound 1 with the receptors of this particular cell line and are discussed later in the manuscript.

3.4. In Silico Assays. Molecular docking is one of the most widely used techniques for *in silico* drug design and drug discovery which involves structure-based virtual screening for identification of particular target protein [35]. The compound was docked against selected proteins using Schrödinger docking module (2021-1). The binding energy of the compound with different receptors is depicted in Table 4, and the 2D interactions are illustrated in Figure 3.

It is observed that the compound shows highest binding efficiency with the receptor 2ETR with binding energy -5.642 kcal/mol. The molecule shows hydrogen bonding at two points: carbonyl oxygen with LYS 105 and one phenolic hydroxyl group with GLU 154. Furthermore, hydrophobic interactions can be observed with amino acids LEU 205, VAL 137, MET 153, ILE 82, PHE 368, TYR 155, and ALA 215. Some positive-charged interactions with LYS 105, LYS 200, and ARG 84 as well as some negative charged interactions with ASP 160, ASP 202, and ASP 216 can also be observed. A polar interaction is shown with the amino acid ASN 203 (Figure 3(a)).

The compound shows moderate binding efficiencies with the receptors 3C3R and 3OBQ as well. In the case of 3C3R, hydrogen bonding can be observed between the two phenolic hydroxyl groups and amino acids GLU 197 and THR 3. Hydrophobic interactions with PHE 4, ALA 2, LEU 201, MET 252, ILE 251, and VAL 297 as well as the polar interactions with THR 3 and ASN 255 could be noted (Figure 3(b)). Considering the receptor 3OBQ, apart from the hydrogen bonds shown between the carbonyl oxygen and SER 143 and one phenyl hydroxyl and TYR 68, pi-pi stacking could also be observed between the aromatic ring and the amino acid TYR 68 (Figure 3(c)).

The molecule shows conventional H-bonding with the amino acid ASP 199 and GLU 203, while showing hydrophobic interactions with PHE 207, PHE 386, PHE 347, MET 274, and ILE 368 of tyrosinase enzyme as depicted in Figure 3(d). In addition to this bonding ability shown by the compound, its skin permeability (-4.48 cm/s) falling between the accepted range of -9.7 cm/s and -3.5 cm/s shows good prospect of being used in skin care industry.

Since the compound shows high binding efficiency for receptor, it can be further studied for this receptor inhibition using various *in vitro* and *in vivo* assays.

To further establish the lead likeliness, the physiochemical properties and pharmacokinetic properties of the compound were evaluated through *in silico* using the comprehensive tool Swiss ADME (Swiss Institute of Bioinformatics) as depicted in Table 5.

Molecule followed different rules like Lipinski, Ghose et al. [36, 37], Veber et al. [38], Egan et al. [39, 40], and Muegge et al. [41] put forth for drug likeliness evaluation with a bioavailability score of 0.55. The compound has topological polar surface area (TPSA) values below 140 Å and can be characterized to have a substantial permeability in the cellular plasma membrane. The compound shows high gastro intestinal absorption with *in silico* absorption percentage of 89.23. The *in silico* absorption percentage was calculated using formula percentage absorption = 109 − (0.345 × TPSA) [42]. The prediction shows it is not P-glycoprotien (P-gp) substrate, making it more suitable as an anticancer agent. The compound occupies the optimal area in SwissADME radar plot (Figure 4). As per the BOILED EGG diagram (Figure 5), the compound has high intestinal absorption as well as is blood brain barrier permeable.

4. Conclusion

The ELF *Phanerochaete sordida* was isolated from the lichen *Bactrospora myriadea* collected from Negombo lagoon, Sri Lanka. Structure of the isolated compound was elucidated as 12,14-dihydroxy-3-methyl-3,4,5,6,7,8,9,10-octahydro-1H-benzo[c][1]oxacyclododecin-1-one (molecular formula: $C_{16}H_{22}O_4$) using ^1H, ^{13}C NMR, DEPT, DQF-COSY, HMBC, HSQC, NOESY, and HR-ESI-MS spectral data. It exhibited high antioxidant activity against $ABTS^{\bullet+}$ in the *in vitro* assay conducted. It also displayed comparable anti-inflammatory, antibacterial activity with moderate tyrosinase inhibition and anticancer activity against oral (CAL-27) cancer cell line. The *in silico* studies done using Schrödinger (2021-1) confirmed the tyrosinase inhibitory and anticancer activity exhibited in *in vitro* assays with similar capacities. The molecule satisfies the key features of drug likeliness like H-bonding, molecular weight, and partition coefficient. The computational pharmacokinetics showed good oral bioavailability and blood-brain permeability as per the BOILED EGG diagram. As the molecule is not a P-gp (plasma glycoprotein) substrate, it can be considered as a good anticancer agent. This study confirms that this compound could be used as a prospective scaffold in the pharmaceutical industry in novel ways other than the already reported ones.

Data Availability

The data used to support the findings of this study are available from the corresponding author upon request.

Conflicts of Interest

The authors declare that they have no conflicts of interest.

Acknowledgments

The authors thank Ms. Patricia Wolseley, Algae, Fungi and Plants Division, Department of Life Sciences, The Natural History Museum, London, for the support rendered in lichen identification and Prof. Mala Amarasinghe, Department of Plant and Molecular Biology, University of Kelaniya, for helping in identification of mangrove host plants. Financial support is provided by the Ministry of Science, Technology and Research, Sri Lanka (grant no: MSTR/TRD/AGR/03/02/07).

Supplementary Materials

File S1: Spectroscopic and chromatographic data of compound 1. *(Supplementary Materials)*

References

[1] A. E. Arnold, J. Miadlikowska, K. L. Higgins et al., "A Phylogenetic Estimation of Trophic Transition Networks for Ascomycetous Fungi: Are Lichens Cradles of Symbiotrophic Fungal Diversification?," *Systematic Biology*, vol. 58, no. 3, pp. 283–297, 2009.

[2] D. Pal, A. K. Nayak, and S. Saha, *Natural Bio-Active Compounds*, M. S. Akhtar, M. K. Swamy, and U. R. Sinniah, Eds., Singapore, Springer Singapore, 2019.

[3] P. A. Paranagama, E. M. K. Wijeratne, A. M. Burns et al., "Heptaketides from Corynespora sp. Inhabiting the cavern beard lichen,usnea cavernosa: first report of metabolites of an endolichenic fungus," *Journal of Natural Products*, vol. 70, no. 11, pp. 1700–1705, 2007.

[4] S. Agrawal, S. K. Deshmukh, M. S. Reddy, R. Prasad, and M. Goel, "Endolichenic fungi: a hidden source of bioactive metabolites," *Journal of Botany*, vol. 134, 186 pages, 2020.

[5] K. A. U. Samanthi, S. Wickramaarachchi, E. M. K. Wijeratne, and P. A. Paranagama, "Two new antioxidant active polyketides from Penicillium citrinum, an endolichenic fungus isolated from Parmotreama species in Sri Lanka," *Journal National Science Foundation Sri Lanka*, vol. 43, no. 2, p. 119, 2015.

[6] K. A. U. Samanthi, S. Wickramarachchi, E. M. K. Wijeratne, and P. A. Paranagama, "Two new bioactive polyketides from Curvularia trifolii, an endolichenic fungus isolated from Usnea sp., in Sri Lanka," *Journal National Science Foundation Sri Lanka*, vol. 43, no. 3, p. 217, 2015.

[7] M. A. T. P. Manthrirathna, R. Kandiah, D. S. Gunasekera et al., "A secondary metabolite with in vitro radical scavenging activity from endolichenic fungus Daldinia eschscholzii found in lichen, Parmotrema sp. in Sri Lanka," *Jounal National Science Foundation Sri Lanka*, vol. 48, no. 2, p. 143, 2020.

[8] S. Santhirasegaram, S. R. Wickramarachchi, R. N. Attanayake et al., "A novel cytotoxic compound from the endolichenic fungus, Xylaria psidii inhabiting the Lichen, Amandinea medusulina," *Natural Product Communications*, vol. 15, no. 7, p. 1934578X2093301, 2020.

[9] H. A. K. Maduranga, W. R. H. Weerasinghe, R. N. Attanayake et al., "Identification of novel bioactive compounds, neurosporalol 1 and 2 from an endolichenic fungus, Neurospora ugadawe inhabited in the Lichen host, Graphis tsunodae Zahlbr. from mangrove ecosystem in Puttalam Lagoon, Sri Lanka," *Journal of Chemistry*, vol. 33, no. 6, 2021.

[10] N. Watanabe, K. Ohkusu, M. Okuda et al., "Phanerochaete sordida as a cause of pulmonary nodule in an immunocompromised patient: a case report," *BMC Infectious Diseases*, vol. 17, no. 1, p. 1, 2017.

[11] E. Yuriev and P. A. Ramsland, "Latest developments in molecular docking: 2010-2011 in review," *Journal of Molecular Recognition*, vol. 26, no. 5, pp. 215–239, 2013.

[12] A. Daina, O. Michielin, and V. Zoete, "SwissADME: a free web tool to evaluate pharmacokinetics, drug-likeness and medicinal chemistry friendliness of small molecules," *Scientific Reports*, vol. 7, no. 1, p. 1, 2017.

[13] A. Borges, M. S. Rosa, G. H. Recchia, J. R. de Queiroz-Silva, E. . A. Bressan, and E. A. Veasey, "CTAB methods for DNA extraction of sweet potato for microsatellite analysis," *Scientia Agricola*, vol. 66, no. 4, pp. 529–534, 2009.

[14] T. J. White, T. Bruns, S. Lee, and J. Taylor, "Amplification and direct sequencing of fungal ribosomal RNA genes for phylogenetics," *PCR Protocols: A Guide to Methods and Applications*, vol. 18, no. 1, p. 315, 1990.

[15] K. Maduranga, R. N. Attanayake, S. Santhirasegaram, G. Weerakoon, and P. A. Paranagama, "Molecular phylogeny and bioprospecting of endolichenic fungi (ELF) inhabiting in the lichens collected from a mangrove ecosystem in Sri Lanka," *PLoS One*, vol. 13, no. 8, p. 1, 2018.

[16] R. Re, N. Pellegrini, A. Proteggente, A. Pannala, M. Yang, and C. Rice-Evans, "Antioxidant activity applying an improved ABTS radical cation decolorization assay," *Free Radical Biology and Medicine*, vol. 26, no. 9-10, pp. 1231–1237, 1999.

[17] S. S. Sakat, A. R. Juvekar, and M. N. Gambhire, "In vitro antioxidant and anti-inflammatory activity of methanol extract of Oxalis corniculata Linn," *Int. J. Pharm. Pharm. Sci*, vol. 2, no. 1, p. 146, 2010.

[18] P. M. Souza, S. T. Elias, L. A. Simeoni et al., "Plants from Brazilian cerrado with potent tyrosinase inhibitory activity," *PLoS One*, vol. 7, no. 11, p. 1, 2012.

[19] I. A. Holder and S. T. Boyce, "Agar well diffusion assay testing of bacterial susceptibility to various antimicrobials in concentrations non-toxic for human cells in culture," *Burns*, vol. 20, no. 5, pp. 426–429, 1994.

[20] M. Paranagama, "A potential green medicine from Sri Lanka against the major cariogenic bacterium, Streptococcus mutans," *Open Access J. Dent. Sci.*, vol. 5, no. 4, 2020.

[21] S. Ansar Ahmed, R. M. Gogal, and J. E. Walsh, "A new rapid and simple non-radioactive assay to monitor and determine the proliferation of lymphocytes: an alternative to [3H]thymidine incorporation assay," *Journal of Immunological Methods*, vol. 170, no. 2, pp. 211–224, 1994.

[22] Ç. Midik, "In Silico Inhibitor Design for Monoamine Oxidase A and B Isozymes," in *Academic Respiratory*, Kadir Has University, 2012.

[23] A. S. Hauser and B. Windshügel, "LEADS-PEP: a benchmark data set for assessment of peptide docking performance," *Journal of Chemical Information and Modeling*, vol. 56, no. 1, pp. 188–200, 2016.

[24] C. M. Chandrasekara, K. D. Weerasinghe, S. Pathirana, and R. U. Piyadasa, "Mangrove Diversity Across Salinity Gradient in Negombo Estuary-Sri Lanka," in *InEnvironmental Geography of South Asia*, pp. 287–304, Springer, Tokyo, 2016.

[25] I. Kamei, H. Suhara, and R. Kondo, "Phylogenetical approach to isolation of white-rot fungi capable of degrading polychlorinated dibenzo-p-dioxin," *Applied Microbiology and Biotechnology*, vol. 69, no. 3, pp. 358–366, 2005.

[26] Y. Xin-Sheng, Y. Ebizuka, H. Noguchi et al., "Structure of arnebinol, a new ANSA-type monoterpenylbenzenoid with inhibitory effect to prostaglandin biosynthesis," *Tetrahedron Letters*, vol. 24, no. 23, pp. 2407–2410, 1983.

[27] S. K. Dey, M. A. Rahman, A. A. Alghamdi, B. V. S. Reddy, and J. S. Yadav, "A Short and efficient approach for the total synthesis of (S)-zearalenone and (R)-de-O-methyllasiodiplodin by using stille and RCM protocols," *European Journal of Organic Chemistry*, vol. 2013, no. 9, pp. 1684–1692, 2016.

[28] E. Ekuadzi, R. A. Dickson, T. C. Fleischer, I. K. Amponsah, D. Pistoriusc, and L. Obererd, "Chemical constituents from Gouania longipetala and Glyphaea brevis," *Natural Product Research*, vol. 28, no. 15, pp. 1210–1213, 2014.

[29] C. L. Lu, W. Zhu, D. M. Wang et al., "Inhibitory effects of chemical compounds isolated from the rhizome of smilax glabra on nitric oxide and tumor necrosis factor-α production in lipopolysaccharide-induced RAW264.7 cell," *Evidence-Based Complementary and Alternative Medicine*, vol. 2015, 2015.

[30] C. S. Jiang, R. Zhou, J. X. Gong et al., "Synthesis, modification, and evaluation of (R)-de- O -methyllasiodiplodin and analogs as nonsteroidal antagonists of mineralocorticoid receptor," *Chemistry Letters*, vol. 21, no. 4, pp. 1171–1175, 2011.

[31] T. Chang, "Natural melanogenesis inhibitors acting through the down-regulation of tyrosinase activity," *Materials*, vol. 5, no. 9, pp. 1661–1685, 2012.

[32] A. Kojima, K. Nakano, K. Wada et al., "Infection of specific strains of Streptococcus mutans, oral bacteria, confers a risk of ulcerative colitis," *Scientific Reports*, vol. 2, no. 1, pp. 1–11, 2012.

[33] G. N. Belibasakis, B. K. Lund, C. K. Weiner et al., "Healthcare challenges and future solutions in dental practice: assessing oral antibiotic resistances by contemporary point-Of-care approaches," *Antibiotics*, vol. 9, no. 11, pp. 1–9, 2020.

[34] J. Wang, S. Gao, S. Wang, Z. Xu, and L. Wei, p. 3441, 2018.

[35] X.-Y. Meng, H.-X. Zhang, M. Mezei, and M. C. Curr, "Molecular docking: a powerful approach for structure-based drug discovery," *Current Computer-Aided Drug Design*, vol. 7, p. 146, 2012.

[36] A. K. Ghose, V. N. Viswanadhan, and J. J. Wendoloski, "Prediction of hydrophobic (lipophilic) properties of small organic molecules using fragmental methods: an analysis of ALOGP and CLOGP methods," *The Journal of Physical Chemistry. A*, vol. 102, no. 21, pp. 3762–3772, 1998.

[37] A. K. Ghose, V. N. Viswanadhan, and J. J. Wendoloski, "A knowledge-based approach in designing combinatorial or medicinal chemistry libraries for drug discovery. 1. A qualitative and quantitative characterization of known drug databases," *Journal of Combinatorial Chemistry*, vol. 1, no. 1, pp. 55–68, 1999.

[38] D. F. Veber, S. R. Johnson, H. Y. Cheng, B. R. Smith, K. W. Ward, and K. D. Kopple, "Molecular properties that influence the oral bioavailability of drug candidates," *Journal of Medicinal Chemistry*, vol. 45, no. 12, pp. 2615–2623, 2002.

[39] W. J. Egan and K. M. Merz, "Prediction of drug absorption using multivariate statistics," *Journal of Medicinal Chemistry*, vol. 43, no. 21, pp. 3867–3877, 2000.

[40] W. J. Egan and G. Lauri, "Prediction of intestinal permeability," *Advanced Drug Delivery Reviews*, vol. 54, no. 3, pp. 273–289, 2002.

[41] I. Muegge, S. L. Heald, and D. Brittelli, "Simple selection criteria for drug-like chemical matter," *Journal of Medicinal Chemistry*, vol. 44, no. 12, pp. 1841–1846, 2001.

[42] F. Azam, A. M. Madi, and H. I. Ali, "Molecular docking and prediction of pharmacokinetic properties of dual mechanism drugs that block MAO-B and adenosine A2A receptors for the treatment of Parkinson's disease," *Journal of Young Pharmacists*, vol. 4, no. 3, pp. 184–192, 2012.